Journal of Alloys and Compounds 694 (2017) 952–958

Contents lists available at ScienceDirect

Journal of Alloys and Compounds

journal homepage: http://www.elsevier.com/locate/jalcom

Upconversion luminescence of a transparent glass ceramics with hexagonal Na(Gd,Lu)F_4 nanocrystals

Guna Krieke*, Anatolijs Sarakovskis, Maris Springis

Institute of Solid State Physics, University of Latvia, 8 Kengaraga str., LV-1063, Riga, Latvia

ARTICLE INFO

Article history:
Received 18 July 2016
Received in revised form
29 August 2016
Accepted 16 October 2016
Available online 17 October 2016

Keywords:
Upconversion
Luminescence
Er^{3+}
Transparent glass ceramics
Oxyfluoride

ABSTRACT

Novel Er^{3+} doped transparent glass ceramics containing hexagonal Na(Gd,Lu)F_4 nanocrystals were prepared from oxyfluoride glasses. The distribution of rare earth ions in the crystalline and glassy phase has been analyzed by X-ray diffraction and erbium luminescence decay kinetics measurement. A strong deviation of rare earth ion content in fluoride nanocrystals in comparison to the base glass has been observed. Preferential incorporation of Gd^{3+} over Lu^{3+} ions in the fluoride lattice leads to the stabilization of hexagonal Na(Gd,Lu)F_4 structure and prevents the formation of cubic fluorite type solid solutions. A considerable enhancement of upconversion luminescence correlates with the formation of hexagonal solid solutions and is attributed to an efficient energy transfer between Er^{3+} ions.

1. Introduction

Transparent oxyfluoride glass ceramics are interesting composites that combine the good chemical and mechanical stability of oxide glasses with the excellent optical properties of fluoride crystals [1–3]. These materials are ideal hosts for rare earth (RE) ions – the low phonon energy of fluorides reduces the non-radiative relaxations.

Among other RE ions, erbium is a widely investigated candidate for infrared to visible upconversion luminescence (UCL) processes due to favorable energy levels and long decay times of its excited states [4]. When introduced to different hosts, the UCL efficiency of erbium depends on its local environment. Significant efforts have been devoted to the investigation of erbium doped β-$NaREF_4$ crystals because they have low phonon energy and low local symmetry of RE ions. Both of these factors contribute to a highly efficient UCL in the materials [5]. Several hexagonal $NaREF_4$ compounds, such as $NaLaF_4$ [6], β-$NaGdF_4$ [7,8] and β-$NaYF_4$ [9] have been successfully precipitated also in aluminosilicate and borosilicate glasses.

Some reports suggest that Er^{3+} doped β-$NaLuF_4$ is a highly efficient host for the UCL and its efficiency can surpass other β-$NaREF_4$ [10,11]. Unfortunately, only its high temperature polymorph α-$NaLuF_4$ has been obtained in the glass ceramics [12–14], although the UCL efficiency of RE doped β-$NaREF_4$ materials is several orders of magnitude higher compared to α-$NaREF_4$ [15].

In aqueous solutions lutetium ions can be introduced in β-$NaREF_4$ lattice by co-precipitation of Na(Gd,Lu)F_4 solid solutions. In these metastable systems Gd^{3+} ions effectively stabilize the hexagonal structure [16]. A similar phenomenon has been observed in oxyfluoride glass ceramics – the introduction of Gd^{3+} in Y^{3+} containing aluminosilicate glasses suppressed the crystallization of α-$NaYF_4$ and a single phase hexagonal $NaREF_4$ was formed [17]. The introduction of rare earth ions with different ionic radii can reduce the local symmetry of the optically active RE and is beneficial for the efficiency of the luminescence [18].

In this work new transparent oxyfluoride glass ceramics containing hexagonal $NaREF_4$ nanocrystals – a solid solution of Er^{3+} doped β-Na(Gd,Lu)F_4 have been prepared. The effects of Lu^{3+} introduction into $NaGdF_4$ lattice on the crystallization and upconversion luminescence of the glass ceramics are investigated.

2. Materials and methods

Glasses with molar composition of $17Na_2O$-7NaF-(8-x)GdF_3-xLuF_3-$7Al_2O_3$-$61SiO_2$ (x = 0–8) doped with 0.1 and 1 mol% Er^{3+} were prepared by melting of analytical grade raw materials. Batches of 9 g were melted in covered corundum crucibles at

* Corresponding author.
E-mail address: guna.krieke@cfi.lu.lv (G. Krieke).

http://dx.doi.org/10.1016/j.jallcom.2016.10.156
0925-8388/

1500 °C for 30 min and casted in stainless steel molds. The high temperature melting leads to changes in the chemical composition of oxyfluoride glasses. The most notable effects are the corrosion of crucible material and decomposition or evaporation of fluorides. A slight increase of Al_2O_3 (less than 1 mol%) can be detected indicating a rather insignificant corrosion of corundum crucibles. However, the fluorine concentration can vary considerably depending on the moisture content of the raw materials. The fluorine content in the glass plays a crucial role in the preparation of glass ceramics. An excess fluorine causes spontaneous crystallization during the melt quenching while significant fluorine loss can completely prevent the formation of nanocrystals. To obtain X-ray amorphous glasses and nanocrystalline glass ceramics, adjustment of Na_2O and NaF ratio might be required.

For the evaluation of RE content in glass ceramics, series of polycrystalline β-Na(Gd,Lu)F_4 were prepared using hydrothermal synthesis followed by a heat treatment. In a typical synthesis a mixture of RE nitrates (0.002 M) were prepared from appropriate amounts of Gd_2O_3 and Lu_2O_3 (99.99%) by dissolving in concentrated HNO_3. The excess HNO_3 was removed by evaporation. The obtained RE nitrates were dissolved in 5 ml of deionized water. A 10 ml of 2.5 M NaF solution was added under vigorous stirring. The pH of the resulting solution was adjusted to 7 with NaOH and the resulting solution was transferred to 25 ml Teflon-lined autoclave, sealed and heated at 200 °C for 24 h. After the reaction, the system was allowed to cool to room temperature naturally. The resulting precipitate was separated by filtration and heat treated at 150 °C for 1 h in He/F_2 gas flow (90% He; 10% F_2) followed by additional heat treatment at 550–650 °C for 1 h in Ar atmosphere. The resulting product was a single phase microcrystalline β-Na(Gd,Lu)F_4.

The differential thermal analysis (DTA) was performed with Shimadzu Corp. DTG-60. The powdered glass samples were heated in corundum crucibles at a rate of 10 K/min in Ar atmosphere. Al_2O_3 powder was used as a reference.

The glass ceramics were obtained by isothermal heat treatment of the precursor glasses. The glasses and glass ceramics are named according to the LuF_3 content in base glass.

X-ray diffraction (XRD) data were measured with PANalytical X'Pert Pro diffractometer using Cu K_α tube operated at 45 kV and 40 mA. The unit cell parameters of β-Na(Gd,Lu)F_4 solid solutions were calculated from XRD patterns using DICVOL [19].

The UCL was excited by pulsed solid state laser Ekspla NT342/3UV (pulse duration – 4 ns) and a temperature controlled continuous wave (CW) laser diode (λ_{em} = 975 nm, variable radiant power up to 1000 mW) from Thorlabs. Luminescence spectra were measured by Andor DU-401-BV CCD camera coupled to Andor SR-303i-B spectrometer. Luminescence decay times were measured by a photomultiplier tube (time resolution better than 20 ns) and digital oscilloscope Tektronix TDS 684A.

3. Results and discussion

Fig. 1 shows DTA curves of oxyfluoride glasses. The characteristic temperatures are summarized in Table 1.

DTA measurements reveal that all characteristic temperatures are rather similar for the glasses with 0–4% LuF_3 and slightly shifted to lower temperatures for the glass with 6% LuF_3.

Glass transition temperature T_g of the glasses with 0–4% LuF_3 lies at approximately 496 °C while for the glass with 6% LuF_3 it is considerably lower (488 °C). The first exothermic effect T_{c1} can only be detected for the glass with the highest LuF_3 content. This effect is attributed to the crystallization of an unknown phase. Two distinct partly overlapping exothermic effects present in all the samples appear at T_{c2} and T_{c3}. According to the XRD data, T_{c2} corresponds to the crystallization of hexagonal $NaREF_4$ while T_{c3} – surface

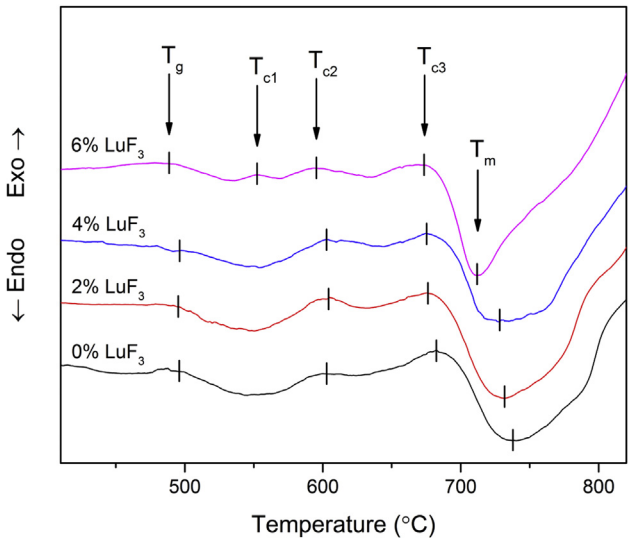

Fig. 1. DTA curves of glasses with 0, 2, 4, and 6 mol% LuF_3.

Table 1
Thermal properties of oxyfluoride glasses.

Sample	T_g (°C)	T_{c1} (°C)	T_{c2} (°C)	T_{c3} (°C)	T_m (°C)
0% LuF_3	496	–	603	682	738
2% LuF_3	495	–	603	676	732
4% LuF_3	496	–	603	675	728
6% LuF_3	488	522	595	673	712

crystallization of aluminosilicates. T_{c3} is followed by an endothermic effect T_m associated with the partial melting of the base glass. The melting temperature of these glasses decrease with the increase of LuF_3 content.

The replacement of GdF_3 with LuF_3 should not lead to significant changes in the connectivity of the glass network, however, it does change the viscosity of the glass melt. There is limited information available about the effect of different rare earth ions on the viscosity of oxyfluoride melts, nevertheless the characteristic melting temperatures of lutetium fluorides are lower than those of gadolinium fluorides [20].

Glass ceramics samples were obtained after the heat treatment of the precursor glasses at 600 °C for 2 h. The glass ceramics with LuF_3 content up to 6% contain only one crystalline phase – hexagonal $NaREF_4$ solid solution (see Fig. 2). The average size of these nanocrystals, estimated using Scherrer equation [21], is 45 ± 4 nm. The small size of β-Na(Gd,Lu)F_4 crystals heat treated at 600 °C for 2 h prevents light scattering, therefore these glass ceramics are highly transparent (see inset of Fig. 2).

When the content of LuF_3 exceeds 7%, additional crystalline phase emerges. The structure of this phase is similar to cubic $NaREF_4$ solid solution, however there seems to be some splitting of plane (220) ($2\theta = 47°$). This could be caused by both the presence of secondary phase and distortion of the fluorite lattice. It should be noted that a complete replacement of GdF_3 by LuF_3 (8% LuF_3 in the base glass) suppresses the formation of hexagonal $NaREF_4$ in the investigated glass ceramics.

The cubic fluorite type compound is observed in all NaF-REF_3 systems except for LaF_3 and CeF_3 [22]. The chemical formula of this compound is often written as stoichiometric α-$NaREF_4$, however, it is a solid solution with variable Na/RE ratio and therefore it should be expressed as α-$Na_xRE_yF_{(x+3y)}$. An increase of the time of the heat treatment reveals that the glass ceramics with high LuF_3 content

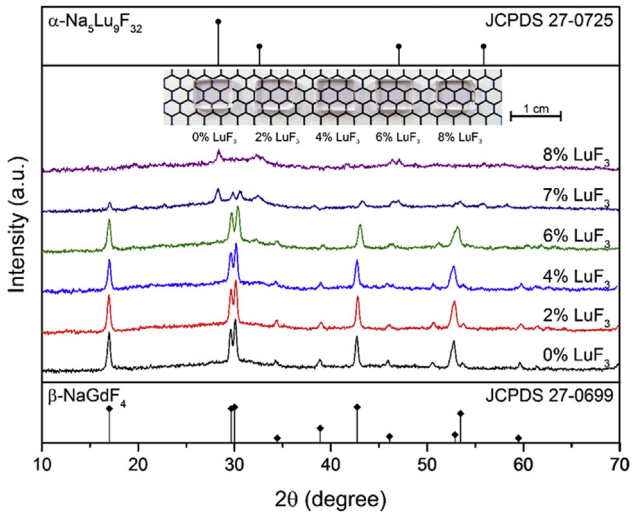

Fig. 2. XRD patterns of glass ceramics with various LuF_3 content (mol%) doped with 1% ErF_3 containing $NaREF_4$ nanocrystals after heat treatment at 600 °C for 2 h. Inset: photograph of respective glass ceramics.

contain two cubic fluorite type phases – possibly, a mixture of two $Na_xRE_yF_{(x+3y)}$ solid solutions with different Na/RE ratio. The region of formation of these solid solutions and the difference between the unit cell parameters of α-$Na_xRE_yF_{(x+3y)}$ with high and low Na/RE ratio increases from Pr^{3+} to Lu^{3+} [22], thus the crystallization of considerably different fluorite type solid solutions in Lu^{3+} containing systems becomes more probable.

According to the DTA data presented previously (see Fig. 1), the crystallization of glass ceramics with high LuF_3 content considerably differs from the glass ceramics with smaller LuF_3 content. The XRD patterns of glass ceramics with 0 and 6% LuF_3 heat treated for 2 h at different temperatures are compared in Fig. 3.

Fig. 3 a) shows XRD pattern of base glass and glass ceramics with 0% LuF_3 heat treated at various temperatures for 2 h. No diffraction peaks can be observed in the precursor glass indicating that it is X-ray amorphous. After the heat treatment sharp diffraction peaks emerge indicating the crystallization of hexagonal $NaGdF_4$. When the temperature of the heat treatment is increased, the peaks become narrow and more intense indicating gradual growth of the fluoride nanocrystals. Similar trend has been observed in other β-$NaGdF_4$ containing glass ceramics [7,8]. The average size of β-$NaGdF_4$ varies from 30 nm (500 °C for 2 h) to 100 nm (700 °C for 2 h) leading to the loss of transparency in the latter. However no significant scattering can be detected for samples heat treated in temperature range 500–600 °C.

The crystallization processes of glass ceramics with high LuF_3 content are more complex. After the heat treatment at 500 °C for 2 h a small fraction of β-$NaREF_4$ with an unidentified compound (marked by asterisk in Fig. 3 b) isostructural to a phase observed in β-$NaYF_4$ containing glass ceramics [9] can be detected. The temperature increase up to 600 °C leads to the formation of single phase hexagonal Na(Gd,Lu)F_4. Further increase of the temperature favors the crystallization of cubic $Na_xRE_yF_{(x+3y)}$. According to the equilibrium diagrams of NaF-REF_3 binary systems, the temperature of polymorphic transition from hexagonal to cubic $NaREF_4$ is considerably higher for $NaGdF_4$ (850 °C) than $NaLuF_4$ (~600 °C) [22], therefore the introduction of Gd^{3+} in the β-$NaLuF_4$ lattice should extend the temperature range, in which the hexagonal phase can be precipitated. In the investigated glass ceramics samples the formation of high temperature α-phase can be detected only in the LuF_3-rich samples. These results suggest that Gd^{3+} ions efficiently stabilize the β-$NaREF_4$ structure in the glass ceramics.

A slight XRD peak shift to higher angles with the increase of LuF_3 content in the glass ceramics indicates a reduction of the interplanar distances and unit cell parameters, suggesting incorporation of ions with smaller ionic radii in the fluoride nanocrystals. In order to estimate the content of RE in the nanocrystals, a series of polycrystalline β-$NaREF_4$ were prepared. The unit cell parameters of the nanocrystals in the glass ceramics and polycrystalline solid solutions with variable GdF_3/LuF_3 ratio are presented in Fig. 4.

A gradual decrease of lattice parameters for both glass ceramics and polycrystalline solid solutions can be detected indicating an incorporation of an ion with smaller ionic radius in the $NaREF_4$ structure.

The polycrystalline β-Na(Gd,Lu)F_4 readily form solid solutions with unlimited solubility. A linear dependence of lattice parameters a = b and c on the LuF_3 content is observed (see Fig. 4b). Both lattice parameters are larger for the glass ceramics than for the polycrystalline materials with the same LuF_3 fraction, suggesting that the RE content in nanocrystals considerably differs from the theoretical estimation, which could be deduced from the rare earth fraction in the base glass. The ionic radii of Gd^{3+}, Er^{3+} and Lu^{3+} for nine-fold coordination expected in β-$NaREF_4$ lattice [23] are 1.107 Å, 1.062 Å and 1.032 Å [24], respectively, therefore the changes in the unit cell can be explained by an incorporation of both Er^{3+} and Lu^{3+} ions in $NaREF_4$ lattice. No significant difference of interplanar distances were detected for glass ceramics doped with 0.1 and 1% ErF_3, probably due to a smaller deviations in ionic radii of Gd^{3+} and Er^{3+} ions. It can be concluded that the contraction of the unit cell with the increase of LuF_3 content in the base glass is mostly due to the replacement of Gd^{3+} by Lu^{3+} in β-Na(Gd,Lu)F_4 lattice.

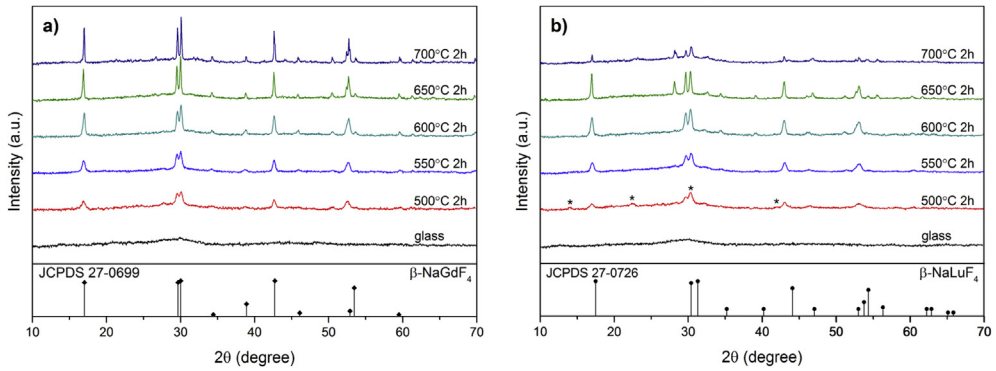

Fig. 3. XRD patterns of the base glass and glass ceramics with a) 0 and b) 6% LuF_3 doped with 1% ErF_3 after appropriate heat treatment. Unidentified metastable phase is marked by asterisk.

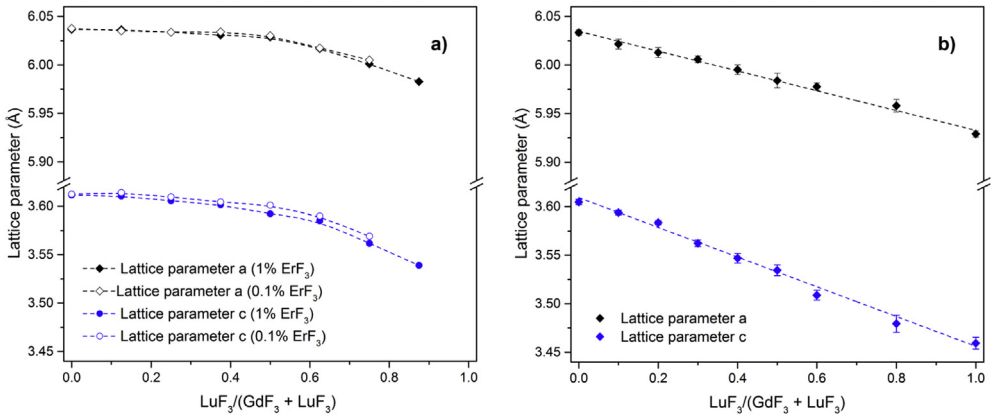

Fig. 4. The change of the lattice parameters a and c a) in glass ceramics doped with 0.1 and 1% ErF_3 and b) polycrystalline β-Na(Gd,Lu)F_4.

In oxyfluoride glass ceramics most of the RE ions are expected to be segregated in the fluoride crystals [1,25,26]. This is one of the greatest advantages of these materials, however the quantitative analysis of the RE distribution is a challenging task. In this study, the LuF_3 content in nanocrystals was estimated by the comparison of lattice parameters of polycrystalline solid solutions with the glass ceramics. The results are shown in Fig. 5.

The Lu^{3+} fraction in β-Na(Gd,Lu)F_4 nanocrystals (experimental fraction) estimated from the XRD data considerably differs from the $LuF_3/(GdF_3+LuF_3)$ ratio in the base glass (theoretical fraction). In these glass ceramics only 45 mol% of Lu^{3+} can be incorporated in β-Na(Gd,Lu)F_4 lattice, which is considerably lower than expected. The preferential binding of larger RE ions with fluorine have been observed in immiscible alkali aluminosilicate oxyfluoride melts [27]. Similar trend can be expected also in oxyfluoride glass ceramics. In fluorine deficient glasses RE (Gd^{3+} and Lu^{3+}) ions are competing for fluorine environment. The larger RE ion (Gd^{3+}) is the first to incorporate in fluorine environment, possibly acting as a nucleating agent. Only when the Gd^{3+} content in the glass is low, a considerable fraction of Lu^{3+} ions can take part in the formation of crystalline phase. This effect can also be applied to the Er^{3+} ions and the preferential incorporation in the fluoride nanocrystals should follow a trend: $Gd^{3+} > Er^{3+} > Lu^{3+}$. However, no clear evidence could be obtained from the XRD data.

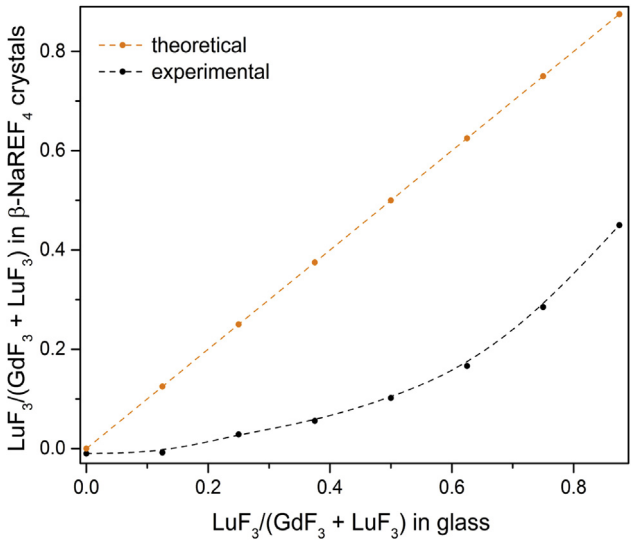

Fig. 5. Theoretical and experimental LuF_3 content in β-$NaREF_4$ nanocrystals.

In order to improve the crystallinity of Lu^{3+} containing glass ceramics, phase separated or partly crystallized Lu^{3+} oxyfluoride glasses are often prepared [12,13,28]. In the Lu^{3+}-rich glasses investigated in the present study, the increase of the fluorine content by variation of Na_2O/NaF ratio resulted in a spontaneous crystallization of the glass during the cooling and improved the crystallinity of the glass ceramics. Nevertheless, only the formation of cubic $Na_xRE_yF_{(x+3y)}$ was detected and the precipitation of stoichiometric β-$NaLuF_4$ nanocrystals in these glasses was not successful.

Fig. 6 a shows room temperature UCL spectra of glass ceramics with various LuF_3 content. Under excitation at 975 nm CW laser three main emission bands of 520, 550 and 660 nm corresponding to $^2H_{11/2} \rightarrow {}^4I_{15/2}$, $^4S_{3/2} \rightarrow {}^4I_{15/2}$ and $^4F_{9/2} \rightarrow {}^4I_{15/2}$ transitions of Er^{3+} attributed to two photon upconversion are detected for all glass ceramics. In addition to these bands violet and blue three photon upconversion emissions from higher emitting states can be observed. All these transitions are summarized in Er^{3+} energy level scheme (Fig. 6 b). A gradual increase of UCL intensity reaching a maximum at 3 mol% LuF_3 in the base glass (corresponding to a 6 mol% LuF_3 in hexagonal nanocrystals) indicate that the formation of β-Na(Gd,Lu)F_4 solid solutions can enhance the UCL efficiency (see Fig. 6 c). With the increase of LuF_3 in the glass ceramics, a rise of red-to-green emission ratio due to increased cross-relaxation between Er^{3+} ions can be observed. The cross-relaxation rate depends on the distance between erbium ions. The cross-relaxation efficiency could be enhanced for two reasons: increase of erbium content in the nanocrystals or decrease of the average distances between rare earth ions due to the replacement of Gd^{3+} by Lu^{3+} leading to the contraction of β-Na(Gd,Lu)F_4 lattice. The change of the red-to-green ratio is gradual but insignificant for the glass ceramics with β-$NaREF_4$ nanocrystals, however a considerable enhancement of the red emission can be observed with the formation of cubic $Na_xRE_yF_{(x+3y)}$ fluorite type phase. From XRD pattern (shown in Fig. 2) one can see that the crystallinity of the cubic phase is low, which could increase the rate of non-radiative multiphonon relaxation or Er^{3+} ions from $^4S_{3/2}$ to $^4F_{9/2}$ in glass matrix and contribute to the enhancement of the red emission.

Fig. 7 shows the UCL decay curves of $^4S_{3/2} \rightarrow {}^4I_{15/2}$ transition in the glass ceramics. With the increase of LuF_3 in the glass composition a gradual decrease of the decay time of the green-emitting state indicate an increase in cross-relaxation processes between Er^{3+} ions in β-$NaREF_4$ nanocrystals. The possible cross-relaxation routes in similar Er^{3+} doped oxyfluoride glass ceramics were reported previously [29].

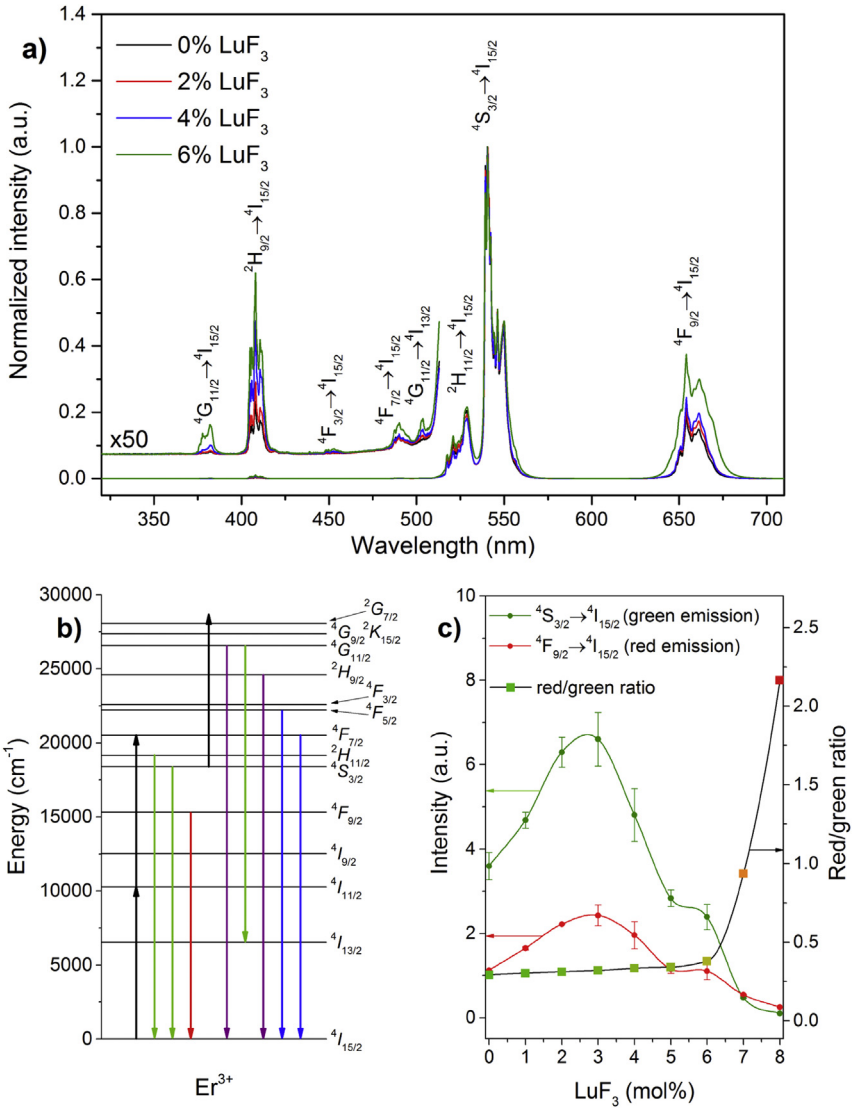

Fig. 6. a) UCL spectra of β-Na(Gd,Lu)F_4 glass ceramics with 0, 2, 4 and 6 mol% LuF_3 doped with 1% ErF_3 excited with 975 nm CW laser, b) energy level scheme of Er^{3+} and c) UCL intensity and red to green luminescence intensity ratio dependence on LuF_3 content in glass. (For interpretation of the references to colour in this figure legend, the reader is referred to the web version of this article.)

Fig. 8 shows the luminescence decay curves of $^4S_{3/2}$ state of Er^{3+} in the glass ceramics doped with 0.1% ErF_3. The low Er^{3+} content prevents efficient cross-relaxation processes, nevertheless a decrease in the lifetime of the emitting state can be detected for the glass ceramics with LuF_3>3 mol%. Both reduction of the average distance between the Er^{3+} ions due to the contraction of β-Na(Gd,Lu)F_4 lattice and an increase of the Er^{3+} content in fluoride crystals can contribute to this effect. The luminescence decay for these glass ceramics can be described as a double-exponential function (see inset in Fig. 8) with two distinct decay rates – fast and slow. This behavior indicates the incorporation of Er^{3+} ions in considerably different environment. A fast luminescence decay suggests a higher non-radiative decay rates induced by non-radiative processes such as multiphonon relaxation or cross-relaxation. In order to determine the origin of the non-exponential behavior of these glass ceramics time-resolved luminescence spectra were measured.

The results are presented in Fig. 9. The luminescence spectrum corresponding to the fast decay (0–0.002 ms) shows broad luminescence bands characteristic to the non-crystalline environment. The sharp luminescence bands detected at longer times (0.01–3 ms) suggest that the corresponding luminescence of Er^{3+} ions appears in the crystalline phase. The relatively high phonon energy of the glass matrix leads to rapid multiphonon relaxation to the lower emitting states shortening the lifetime of the green emission, while the Er^{3+} ions in the lower phonon energy crystalline environment favor the radiative decay. Thus, we can conclude that the fast component in the decay curves is caused by the luminescence of Er^{3+} ions in glass matrix and the slow component is the result of luminescence of Er^{3+} located in β-Na(Gd,Lu)F_4. The comparison of the luminescence decay ratio of the fast and slow component can be used to qualitatively analyze the Er^{3+} fraction in glass and crystalline phase. An obvious increase of the relative intensity of the slow component with the increase of LuF_3 content up to 3 mol% can be observed in the insets of Figs. 8 and 9 suggesting an increase of Er^{3+} ion content in the crystalline phase. A further increase of the LuF_3 content reveals a rise of the fast-to-slow luminescence integral intensity

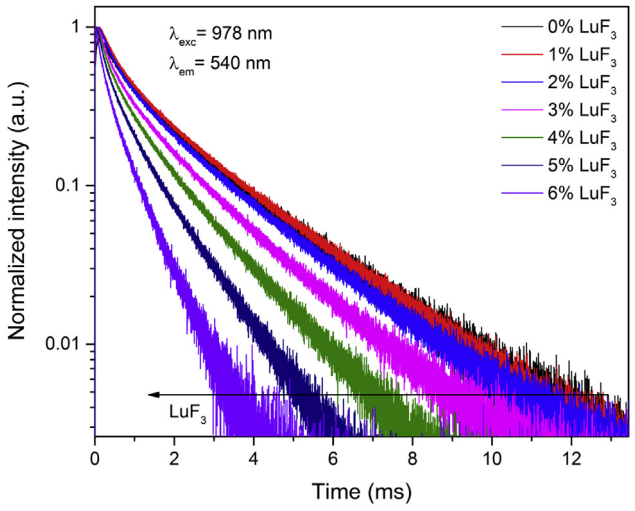

Fig. 7. UCL decay curves of Er^{3+} green emission (monitored at $\lambda_{em} = 540$ nm, excited with $\lambda_{exc} = 978$ nm) in β-$NaREF_4$ containing glass ceramics doped with 1% ErF_3. (For interpretation of the references to colour in this figure legend, the reader is referred to the web version of this article.)

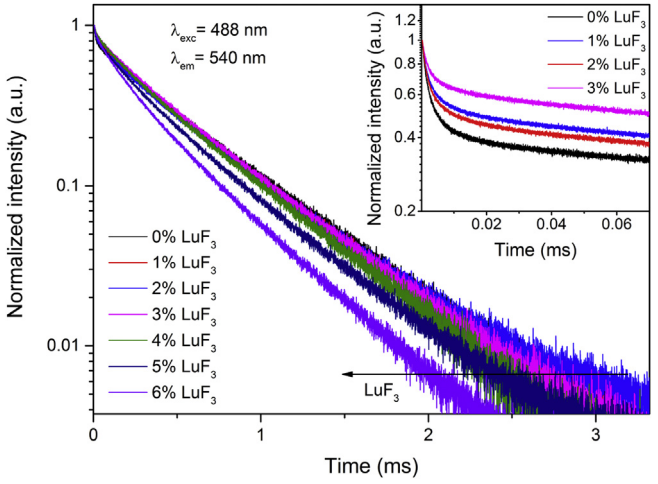

Fig. 8. Luminescence decay curves of Er^{3+} green emission (monitored at $\lambda_{em} = 540$ nm, excited with $\lambda_{exc} = 488$ nm) in glass ceramics with 0–6% LuF_3 doped with 0.1% ErF_3. Inset: enlarged initial part of the decay curves. (For interpretation of the references to colour in this figure legend, the reader is referred to the web version of this article.)

ratio. This phenomenon could be caused by the decrease of the Er^{3+} content in the crystalline phase, however it is highly unlikely due to the observed increase of the cross-relaxation rate in β-$NaREF_4$ nanocrystals. The most probable explanation is the reduction of the integral intensity of slow component in luminescence decay curves caused by cross-relaxation and as the result increasing the relative intensity fast and slow component intensity ratio.

The results suggest that in the mixed rare earth oxyfluoride glasses preferential incorporation of rare earth ions with larger ionic radii plays an important role in the crystallization of the glass and has a significant impact on the UCL processes. The replacement of Gd^{3+} ions with Lu^{3+} leads to the increase of both Lu^{3+} and Er^{3+} content in the fluoride nanocrystals, decreasing the average distance between Er^{3+} ions and improving the energy transfer and cross-relaxation processes in these materials.

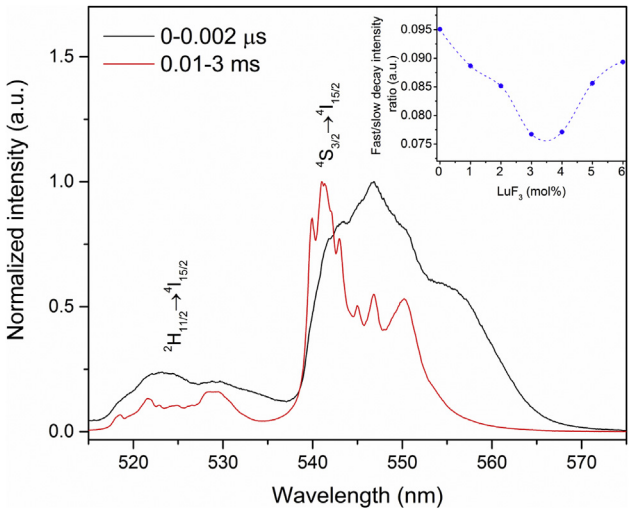

Fig. 9. Time-resolved spectra of glass ceramics with 0.1% ErF_3 corresponding to the fast (0–0.002 ms) and slow (0.01–3 ms) components of luminescence decay excited at 488 nm. Inset: Fast and slow luminescence integral intensity ratio in glass ceramics.

4. Conclusions

For the first time Er^{3+} doped transparent glass ceramics with hexagonal Na(Gd,Lu)F_4 nanocrystals has been prepared using melt-quenching and subsequent heat treatment. The Gd^{3+} ions are predominantly incorporated in the fluoride nanocrystals, effectively stabilizing the hexagonal structure and preventing the formation of cubic $NaLuF_4$. An efficient upconversion luminescence of Er^{3+} ions has been observed under infrared excitation. With the increase of LuF_3 content in nanocrystals a gradual decrease of unit cell dimensions and lifetimes Er^{3+} emitting states has been detected indicating a reduction of average distance between erbium ions in the nanocrystals. The most efficient upconversion luminescence has been detected for Er^{3+} doped β-Na(Gd,Lu)F_4 glass ceramics with approximately 6 mol% LuF_3 incorporated in the hexagonal lattice, however, the maximum Lu^{3+} ions concentration reaching 45 mol% could be obtained.

Acknowledgments

This work was supported by National Research Program IMIS^2. G.K. gratefully acknowledges the financial support from the Foundation of University of Latvia — Arnis Riekstins "MikroTik" donation.

References

[1] P.P. Fedorov, A.A. Luginina, A.I. Popov, Transparent oxyfluoride glass ceramics, J. Fluor. Chem. 172 (Apr. 2015) 22–50.
[2] D. Chen, W. Xiang, X. Liang, J. Zhong, H. Yu, M. Ding, H. Lu, Z. Ji, Advances in transparent glass–ceramic phosphors for white light-emitting diodes—A review, J. Eur. Ceram. Soc. 35 (3) (Mar. 2015) 859–869.
[3] M. Ferrari, M.J. Pascual, G.C. Righini, Glass-ceramics: a class of nanostructured materials for photonics, La Riv. del Nuovo Cim. 38 (7–8) (2015) 311–369.
[4] A. Shalav, B.S. Richards, M.A. Green, Luminescent layers for enhanced silicon solar cell performance: up-conversion, Sol. Energy Mater. Sol. Cells 91 (2007) 829–842 no. February.
[5] C. Renero-Lecuna, R. Martin-Rodriguez, R. Valiente, J. Gonzalez, F. Rodriguez, K.W. Krämer, H.U. Güdel, Origin of the high upconversion green luminescence efficiency in β-$NaYF_4$:2%Er^{3+}, 20%Yb^{3+}, Chem. Mater. 23 (15) (Aug. 2011) 3442–3448.
[6] A. de Pablos-Martín, G.C. Mather, F. Muñoz, S. Bhattacharyya, T. Höche, J.R. Jinschek, T. Heil, A. Durán, M.J. Pascual, Design of oxy-fluoride glass-ceramics containing $NaLaF_4$ nano-crystals, J. Non. Cryst. Solids 356 (52–54) (Dec. 2010) 3071–3079.
[7] A. Herrmann, M. Tylkowski, C. Bocker, C. Rüssel, Cubic and hexagonal NaGdF4

crystals precipitated from an aluminosilicate Glass: preparation and luminescence properties, Chem. Mater. 25 (14) (Jul. 2013) 2878–2884.
[8] F. Xin, S. Zhao, L. Huang, D. Deng, G. Jia, H. Wang, S. Xu, Up-conversion luminescence of Er^{3+}-doped glass ceramics containing β-$NaGdF_4$ nanocrystals for silicon solar cells, Mater. Lett. 78 (Jul. 2012) 75–77.
[9] A. Sarakovskis, G. Krieke, Upconversion luminescence in erbium doped transparent oxyfluoride glass ceramics containing hexagonal $NaYF_4$ nanocrystals, J. Eur. Ceram. Soc. 35 (13) (Nov. 2015) 3665–3671.
[10] E. He, H. Zheng, W. Gao, Y. Tu, Y. Lu, G. Li, Investigation of upconversion and downconversion fluorescence emissions from β-$NaLn1F_4$:Yb^{3+}, $Ln2^{3+}$ (Ln1 = Y, Lu; Ln2 = Er, Ho, Tm, Eu) hexagonal disk system, Mater. Res. Bull. 48 (9) (2013) 3505–3512.
[11] F. Shi, J. Wang, X. Zhai, D. Zhao, W. Qin, Facile synthesis of β-$NaLuF_4$: Yb/Tm hexagonal nanoplates with intense ultraviolet upconversion luminescence, CrystEngComm 13 (11) (2011) 3782.
[12] D. Chen, Y. Zhou, Z. Wan, P. Huang, H. Yu, H. Lu, Z. Ji, Enhanced upconversion luminescence in phase-separation-controlled crystallization glass ceramics containing Yb/Er(Tm): NaLuF4 nanocrystals, J. Eur. Ceram. Soc. 35 (7) (2015) 2129–2137.
[13] D. Chen, Z. Wan, Y. Zhou, P. Huang, Z. Ji, Ce^{3+} dopants-induced spectral conversion from green to red in the Yb/Ho: NaLuF4 self-crystallized nano-glass-ceramics, J. Alloys Compd. 654 (2016) 151–156.
[14] Y. Wei, X. Liu, X. Chi, R. Wei, H. Guo, Intense upconversion in novel transparent $NaLuF_4$:Tb^{3+}, Yb^{3+} glass–ceramics, J. Alloys Compd. 578 (Nov. 2013) 385–388.
[15] J.L. Sommerdijk, Influence of host lattice on the infrared-excited visible luminescence in Yb^{3+}, Er^{3+}-doped fluorides, J. Lumin. 6 (1973) 61–67.
[16] S.V. Kuznetsov, A. a. Ovsyannikova, E. a. Tupitsyna, D.S. Yasyrkina, V.V. Voronov, N.I. Batyrev, L.D. Iskhakova, V.V. Osiko, P.P. Fedorov, Phase formation in LaF_3–$NaGdF_4$, $NaGdF_4$–$NaLuF_4$, and $NaLuF_4$–$NaYF_4$ systems: synthesis of powders by co-precipitation from aqueous solutions, J. Fluor. Chem. 161 (May 2014) 95–101.
[17] S. Zhao, X. Sun, X. Wang, L. Huang, Y. Fei, S. Xu, The influence of phase evolution on optical properties in rare earth doped glass ceramics containing $NaYF_4$ nanocrystals, J. Eur. Ceram. Soc. 35 (15) (Dec. 2015) 4225–4231.
[18] G. Liu, Advances in the theoretical understanding of photon upconversion in rare-earth activated nanophosphors, Chem. Soc. Rev. 44 (6) (2015) 1635–1652.
[19] A. Boultif, D. Louër, D. Loueer, Indexing of powder diffraction patterns for low-symmetry lattices by the successive dichotomy method, J. Appl. Crystallogr. 24 (6) (Dec. 1991) 987–993.
[20] R.E. Thoma, Phase diagrams of binary and ternary fluoride systems, in: Advances in Molten Salt Chemistry, Springer US, Boston, MA, 1975, pp. 275–455.
[21] A. Monshi, Modified scherrer equation to estimate more accurately nano-crystallite size using XRD, World J. Nano Sci. Eng. 02 (03) (2012) 154–160.
[22] R. Thoma, H. Insley, G. Hebert, The sodium fluoride-lanthanide trifluoride systems, Inorg. Chem. 1005 (1966) 1222–1229.
[23] J.H. Burns, Crystal structure of hexagonal sodium neodymium fluoride and related compounds, Inorg. Chem. 4 (6) (1965) 881–886.
[24] R.D. Shannon, Revised effective ionic radii and systematic studies of interatomic distances in halides and chalcogenides, Acta Crystallogr. Sect. A 32 (1976) 751–767.
[25] A. de Pablos-Martin, C. Patzig, T. Höche, A. Duran, M.J. Pascual, Distribution of thulium in Tm^{3+}-doped oxyfluoride glasses and glass-ceramics, CrystEngComm 15 (35) (2013) 6979.
[26] D. Chen, Z. Wan, Y. Zhou, Y. Chen, H. Yu, H. Lu, Z. Ji, P. Huang, Lanthanide-activated $Na_5Gd_9F_{32}$ nanocrystals precipitated from a borosilicate glass: phase-separation-controlled crystallization and optical property, J. Alloys Compd. 625 (Mar. 2015) 149–157.
[27] I.V. Veksler, A.M. Dorfman, M. Kamenetsky, P. Dulski, D.B. Dingwell, Partitioning of lanthanides and Y between immiscible silicate and fluoride melts, fluorite and cryolite and the origin of the lanthanide tetrad effect in igneous rocks, Geochim. Cosmochim. Acta 69 (11) (Jun. 2005) 2847–2860.
[28] J. Cao, X. Wang, X. Li, Y. Wei, L. Chen, H. Guo, Enhanced emissions in Tb3+-doped oxyfluoride scintillating glass ceramics containing KLu_2F_7 nano-crystals, J. Lumin. 170 (2015) 207–211.
[29] G. Krieke, A. Sarakovskis, Crystallization and upconversion luminescence of distorted fluorite nanocrystals in Ba^{2+} containing oxyfluoride glass ceramics, J. Eur. Ceram. Soc. 36 (7) (Jun. 2016) 1715–1722.